Research Paper
Computational Methods for Differential Equations
http://cmde.tabrizu.ac.ir
Vol. *, No. *, *, pp. 1-23
DOI:10.22034/cmde.2026.69373.3413

Efficient numerical algorithms for pricing complex financial derivatives in fractional Black-Scholes models

Hamed Payandehdoost Masouleh[1] **and Mojgan Esmailzadeh**[2,*]

[1]Department of Accounting, BaA.C., Islamic Azad University, Bandar Anzali, Iran.

[2]Department of Applied Mathematics, BaA.C., Islamic Azad University, Bandar Anzali, Iran.

Abstract

In this study, we examine the generalized distributed-order fractional Black-Scholes equation through two distinct numerical approaches. The temporal derivative is approximated using a scheme analogous to the classical $L1$ method, ensuring accuracy in capturing fractional dynamics. For the spatial discretization, we employ two finite difference techniques alongside a collocation method based on Romanovski-Jacobi polynomials, which provides enhanced flexibility in handling complex boundary behaviors. The numerical experiments confirm the high accuracy and robustness of the proposed methods in solving financial models governed by fractional dynamics. Each approach exhibits distinct strengths: the collocation method achieves superior accuracy, while the finite difference schemes offer greater computational efficiency. Moreover, the use of an implicit formulation guarantees numerical stability even with larger time steps, making the method particularly suitable for long-term financial simulations.

Keywords. Generalized Fractional distributed–order derivatives, Black–Scholes model, Finite difference method, Romanovski-Jacobi polynomials, Collocation method.

2010 Mathematics Subject Classification. 65M22, 65M70, 65M99.

1. Introduction

The Black-Scholes (B-S) model is a crucial instrument for option pricing (OP) in financial markets. This model is represented by a parabolic partial differential equation that captures the dynamics of financial derivatives, particularly options on equity shares. The formulation of the equation involves the application of Itô's calculus, under the premise that the value of the underlying asset evolves over time according to a stochastic differential equation. This evolution is further influenced by specific assumptions about the financial market environment [7].

A fundamental principle of the B-S model is the concept of arbitrage-free reasoning, which ensures that there are no opportunities for riskless profit. This model has found extensive application in the pricing of options across a wide range of commodities and various payoff structures. Its robustness and versatility have made it a cornerstone in the field of financial mathematics, providing a theoretical foundation for understanding and predicting the behavior of options in diverse market conditions. Moreover, the B-S model's ability to incorporate market volatility and other financial parameters has enhanced its utility in real-world scenarios. By enabling the accurate pricing of options, the model helps investors and financial institutions manage risk and make informed decisions. The widespread adoption of the B-S model underscores its significance in both academic research and practical financial operations [32].

In the academic literature, numerous methods have been proposed for valuing European and American options. For example, Company et al. [13] introduced a finite-difference numerical scheme tailored for Black-Scholes (B-S) equations, which are used to model illiquid markets where the price impact in the underlying asset market influences the replication of a European contingent claim. Lesmana and Wang [26] explored a dependable computational method for solving the B-S model. In another study [15], the authors presented the lattice procedure for option pricing (OP).

Received: 28 September 2025; Accepted: 09 May 2026.
∗ Corresponding author. Email: Mojgan.Esmailzadeh@iau.ac.ir.

Hull and White [20] employed a control variate method for OP. Valkov [44] developed a fitted finite-volume technique to examine a generalized B-S model and conducted a convergence analysis of a fitted finite-volume element procedure that maintains positivity. Cen and Le [10, 11] utilized a robust numerical approach to address the linear complementarity problem arising from OP and proposed an implicit time-stepping procedure for a generalized B-S equation. The fitted finite-volume techniques and implicit time-stepping procedures contribute to the stability and convergence of numerical solutions, ensuring that the models remain reliable under various market scenarios. These advancements not only enhance the theoretical understanding of option pricing but also have practical implications for financial markets, enabling better risk management and investment strategies. Additionally, Rao [40] introduced a numerical scheme to approximate option prices for various option styles governed by the generalized Black-Scholes (B-S) equation in its degenerate form. In studies [5, 45], the authors proposed a finite volume method to discretize the B-S equation arising from option pricing (OP). In [22, 23], collocation procedures based on uniform cubic B-splines and non-uniform B-splines were developed for the numerical solution of the generalized B-S partial differential equation, achieving second-order convergence with respect to both variables. In [4], an implicit numerical scheme for solving the time-fractional B-S model was discussed. Furthermore, Prathumwan and Trachoo [39] employed the Localized Homotopy Perturbation Method (LHPM) for the fractional-order B-S equation. Roul and Goura [41] implemented a high-order numerical procedure with a uniform mesh for the generalized B-S equation. Chen et al. [4] proposed a solution to the generalized B-S equation utilizing the Laguerre neural network. These diverse methodologies underscore the extensive research dedicated to enhancing the accuracy and efficiency of option pricing models. The finite volume methods and collocation procedures offer robust numerical solutions, particularly useful in handling complex market conditions and nonlinearities. Implicit numerical schemes and LHPM contribute to the stability and convergence of solutions, ensuring reliability under various market scenarios. The Galerkin-based procedures and high-order numerical methods provide sophisticated techniques for addressing the intricacies of the B-S and Heston models. The use of neural networks, such as the Laguerre neural network, introduces advanced computational approaches that leverage machine learning for solving the generalized B-S equation. These advancements not only deepen the theoretical understanding of option pricing but also have significant practical implications. They enable better risk management and investment strategies in financial markets, demonstrating the critical role of numerical methods in modern financial mathematics. In conclusion, the Black-Scholes (B-S) equation is an essential model for option pricing (OP) in financial markets. It is extensively utilized, and numerous numerical methods have been suggested in the literature to value both European and American options. These methods offer various applications and benefits, and researchers continue to develop new techniques to enhance the accuracy and efficiency of OP.

However, as stated in [12], empirical evidence shows that the classical Black-Scholes model cannot capture certain price characteristics, such as periods of constant prices often seen in emerging markets with low transaction volumes. These constant periods resemble trapping events where subdiffusive particles become immobilized, further justifying the use of time-fractional Black-Scholes models. Additionally, [24] demonstrated that the value of European-style options satisfies a partial integro-differential equation in time-to-maturity, with the time-to-maturity derivative being fractional. Since 1976, Levy processes have been introduced to model the skewness and fat tails of log returns, which the geometric Brownian motion (GBM) model of Black-Scholes does not account for. Subsequently, stochastic volatility models were developed to address volatility clustering and the leverage effect, significantly enhancing the modeling capabilities of the Black-Scholes equation. Notably, [28] showed that the fractional Black-Scholes formula, which replaces Brownian motion in the GBM formula with fractional Brownian motion, provided better estimates for high volatility cases using foreign exchange call option price data from China Merchants Bank. Building on this GBM formula with fractional Brownian motion, [8] derived the time-fractional Black-Scholes equations. The success of the fractional Black-Scholes equation in modeling high volatility cases may be attributed to the effectiveness of fractional operators in explaining the hereditary and memory characteristics of various substances, making fractional order processes a promising approach for accounting for high volatility in stock markets [21, 31]. Fractional Black-Scholes models have garnered increasing attention due to significant contributions by researchers such as Masouleh and Esmailzadeh [38] and Cartea et al. [18]. These models assume that the dynamics of equity prices follow jump-diffusion processes or infinite activity Lévy processes, leading to financial derivative price dynamics that satisfy fractional partial differential equations (FPDEs).

The numerical solution of advanced financial models, particularly those incorporating non-local operators, continues to benefit from innovations in computational mathematics. Recent studies demonstrate this trend through diverse approaches. For instance, the application of spectral techniques is exemplified in the work on 'Simulating and pricing CAT bonds using the spectral method based on Chebyshev basis' [3], highlighting the effectiveness of orthogonal polynomial expansions for complex stochastic pricing problems. Furthermore, enhancing discretization schemes remains a key focus, as seen in the development of an 'Approximate price of the option under discretization by applying fractional quadratic interpolation' [34], which improves accuracy through specialized approximation techniques. Closely related to the present financial context, the rigorous 'convergence investigation of a numerical scheme for the tempered fractional Black-Scholes model arising in European double barrier option' pricing [2] provides a valuable framework for analyzing schemes applied to fractional derivatives with barriers. Building upon these developments, our work introduces and analyzes numerical methods for the more generalized distributed-order fractional framework, extending the computational toolkit for pricing complex derivatives under models with memory effects.

The developed numerical framework is particularly pertinent for real-world financial modeling, where capturing persistent volatility clusters and long-range memory effects is essential for accurate option pricing and risk management under market stress.

In this study, we investigate an innovative model termed the generalized distributed-order time-fractional Black-Scholes equation. This advanced model is specifically designed to capture the dynamics of pricing European double barrier options. The equation incorporates the complexities of and distributed-order fractional derivatives, providing a more accurate and flexible framework for financial modeling. By leveraging this model, we aim to enhance the precision of option pricing, particularly in scenarios where traditional models fall short. The detailed formulation and implications of this equation are discussed as follows [47]:

$$\left(\partial_t + \theta^{\gamma}\partial_t^* + \mathcal{L}_x\right) v(x,t) = f(x,t),\ x \in (\alpha_1, \alpha_2),\ t \in (0,T], \tag{1.1}$$

with homogeneous Dirichlet boundary conditions and the initial condition

$$v(x,0) = v_0(x), \quad \alpha_1 \le x \le \alpha_2, \tag{1.2}$$

where $\mathcal{L}_x = -a\partial_{xx} + b\partial_x + c$. Here $\rho \ge 0$ is the balance between the derivative of the integer-order and of the distribution-order, $a = \frac{\sigma^2}{2}$, $b = a - r$, $c = r$, $r \ge 0$ is the risk-free rate, $\sigma \ge 0$ is the volatility, $f \in C[\alpha_1, \alpha_2] \times C[0,T]$ and $v_0 \in C^2[\alpha_1, \alpha_2]$ are considered as known functions. Here, ${}^{\gamma}\partial_t^*$ denotes the generalized distributed-order differential operator which is defined as follow

$${}^{\gamma}\partial_t^* v(x,t) = \int_{\beta_*}^{\beta^*} \gamma(\beta, x, t)\partial_t^{\beta} v(x,t) d\beta, \tag{1.3}$$

where $\gamma(\beta, x, t)$ is known density function and

$$\partial_t^{\beta} v(x,t) = \frac{t^{-\beta}}{\Gamma(1-\beta)} * \partial_t v(x,t) = \frac{1}{\Gamma(1-\beta)} \int_0^t (t-s)^{-\beta} \frac{\partial v(x,s)}{\partial s} ds,$$

where $*$ represents the convolution defined as. The generalized fractional distributed-order Black-Scholes model has garnered significant interest recently due to its ability to generalize previous models [4, 30, 36, 37, 42, 48]. Despite its potential, numerical solutions for this model have been scarce. In this article, we address this gap by providing a numerical solution.

1.1. **Economic Interpretation and Market Calibratability.** One of the critical advantages of the generalized distributed-order time-fractional Black-Scholes model is its ability to encode complex market microstructures through its fractional parameters. In this subsection, we provide an economic interpretation of the distributed-order parameters and outline a practical calibration framework linking them to observable market quantities [14].

The distributed-order fractional operator ${}^{\gamma}\partial_t^*$ introduced in Eq. (1.3) generalizes the concept of temporal memory in asset price dynamics. The key parameters admit the following financial interpretations [29]:

- The fractional order $\beta \in (0,1)$: This parameter serves as an index of market memory persistence. When $\beta \to 1$, the operator reduces to the classical first-order derivative, corresponding to the efficient market hypothesis with no memory. Conversely, values of $\beta < 1$ capture long-range dependence and sub-diffusive behavior, often

observed in emerging markets or during periods of financial stress where price adjustments are delayed due to illiquidity or behavioral frictions [43].

- The density function $\gamma(\beta, x, t)$: This function represents the heterogeneity of market participants. Financial markets comprise agents with diverse trading horizons-ranging from high-frequency traders (short memory) to institutional investors (long memory). The distribution $\gamma(\beta)$ quantifies the relative weight of these different time-scales in the aggregate price formation process [9]. A peak in $\gamma(\beta)$ near $\beta \approx 0.5$, for instance, would indicate a market dominated by agents exhibiting strong rough volatility characteristics.
- The balance parameter θ: This coefficient modulates the relative contribution of the classical diffusion term versus the fractional memory term. A larger θ implies that non-local (memory) effects play a more dominant role in option pricing, which is particularly relevant for long-maturity options or assets with pronounced path-dependence [49].

To ensure the model's practical utility, we propose a calibration procedure that maps the fractional parameters $\Theta = \{\theta, \sigma, \gamma(\cdot)\}$ to observable option prices. Let $\{P^{\text{mkt}}(K_i, T_i)\}_{i=1}^N$ denote the market prices of European options with strikes K_i and maturities T_i. The calibration problem is formulated as a regularized least-squares optimization [27]:

$$\min_{\Theta} \mathcal{J}(\Theta) := \sum_{i=1}^{N} w_i \left(P^{\text{model}}(K_i, T_i; \Theta) - P^{\text{mkt}}(K_i, T_i)\right)^2 + \lambda \|\Theta\|_2^2, \tag{1.4}$$

where P^{model} is computed via the numerical scheme developed in section 2, w_i are liquidity-based weights, and $\lambda > 0$ is a Tikhonov regularization parameter to mitigate overfitting and ensure the well-posedness of the inverse problem.

The optimization is performed using the Levenberg-Marquardt algorithm, with gradients computed via adjoint-state methods for efficiency. This framework allows the distributed-order parameters to be inferred directly from the implied volatility surface, thereby establishing a concrete link between the abstract fractional operators and observable market quantities such as the volatility smile and term structure [16].

To contextualize the contributions of the generalized distributed-order model, we compare its financial behavior with three well-established alternatives: the Heston stochastic volatility model, the Merton jump-diffusion model, and the rough volatility framework. This comparison highlights the unique flexibility and computational advantages of our approach.

The Heston model [19] introduces a mean-reverting stochastic variance process to capture the volatility smile. While effective, it requires simulating two correlated stochastic differential equations, which increases computational complexity, especially for path-dependent options like double barrier contracts.

Flexibility: Our distributed-order model achieves comparable flexibility in fitting the volatility surface through the memory kernel $\gamma(\beta)$, without explicitly modeling stochastic variance. The fractional derivative inherently captures volatility clustering and mean-reversion effects through its non-local temporal structure [9].

Computational Efficiency: For barrier options, our PDE-based approach avoids the Monte Carlo simulations typically required for the Heston model, leading to faster and more stable pricing, particularly near barrier levels where simulation methods suffer from high variance.

The Merton model [33] incorporates discontinuous jumps to account for fat tails and sudden market movements. While jumps effectively model extreme events, they introduce an integro-differential equation (PIDE) that is numerically challenging to solve, especially with barriers.

Numerical Tractability: By retaining a pure PDE structure (Eq. (1.1)), our model avoids the computational burden of evaluating integral terms at each time step, simplifying the implementation of boundary conditions for double barrier options.

Recent empirical studies [17] suggest that volatility exhibits "rough" behavior with a Hurst exponent $H \approx 0.1$. Rough volatility models, while highly accurate, often rely on non-Markovian simulations that are computationally intensive [6].

Unification: The proposed distributed-order framework naturally encompasses rough volatility as a special case. By concentrating the density $\gamma(\beta)$ around $\beta = H + 0.5$, our model replicates the rough scaling laws. However, the distributed-order formulation offers greater generality, allowing the model to adapt to markets that transition between rough and classical regimes over time.

Table 1. Qualitative comparison of financial models for barrier option pricing.

Feature	Proposed Model	Heston [19]	Merton [33] / Rough [17]
Volatility Smile	Captured via $\gamma(\beta)$	Captured via stochastic variance	Captured via jumps / rough kernel
Memory Effects	Explicit (Distributed-order)	Implicit (Mean-reversion)	Implicit (Roughness)
Numerical Method	PDE (Finite Difference/Spectral)	PDE / Monte Carlo	PIDE / Monte Carlo
Barrier Handling	Direct (Dirichlet BC)	Challenging (Simulation)	Complex (Integral BC)
Parameter Count	Moderate (Functional γ)	Moderate (5-6 params)	High (Jump params / Rough H)

Table 2. Pricing errors for different models on S&P 500 option data.

Model	RMSE ($)	MAPE (%)
Classical Black-Scholes [7]	4.82	12.5%
Distributed-Order Fractional (Proposed)	**1.35**	**3.2%**

Parameter Stability: Unlike single-order fractional models that may require time-varying β to fit different maturities, our distributed-order approach can fit the entire term structure with a single, time-invariant density function $\gamma(\beta)$, enhancing parameter stability and interpretability [46].

Table 1 summarizes the key distinctions. Our model offers a balanced trade-off between descriptive power, numerical tractability, and economic interpretability, making it particularly suitable for pricing exotic options in markets with complex memory effects.

To quantify the model's performance, we compute the Root Mean Square Error (RMSE) and the Mean Absolute Percentage Error (MAPE) between model prices and market prices:

$$\text{RMSE} = \sqrt{\frac{1}{N}\sum_{i=1}^{N}\left(P_i^{\text{model}} - P_i^{\text{mkt}}\right)^2}, \quad \text{MAPE} = \frac{100\%}{N}\sum_{i=1}^{N}\left|\frac{P_i^{\text{model}} - P_i^{\text{mkt}}}{P_i^{\text{mkt}}}\right|. \tag{1.5}$$

As shown in Table 2, the proposed model reduces the pricing error by approximately 70% compared to the classical model. This significant improvement demonstrates that the distributed-order fractional framework is not merely a theoretical generalization, but a practical tool capable of enhancing pricing accuracy for exotic derivatives.

The paper is organized as follows: In section 2, we examine a solution method for solving problem (1.1)–(1.2) and its error analysis using finite difference techniques. Section 4 presents some numerical examples, with results depicted through figures to showcase the method's effectiveness. Finally, section 5 concludes the paper with a summary of our findings and suggestions for future research directions.

2. Numerical Methods

In this section, we will solve Problem (1.1)–(1.2) numerically using two methods. First, we present an approximation for the fractional derivative of the distribution order. Then, for the spatial approximation, we first present a collocation method based on Romanovski-Jacobi polynomials. Finally, we will use a central finite difference approximation for comparison.

2.1. Romanovski-Jacobi collocation method.

Let $x_l = \alpha_1 + l\Delta x$, $l = 0, 1, \ldots, L$, $\Delta x = \frac{\alpha_2 - \alpha_1}{L}$, $t_n = n\Delta t$, $n = 0, 1, \ldots, N$, $\Delta t = \frac{T}{N}$, $t_{n+\frac{1}{2}} = t_n + \frac{1}{2}\Delta t$ and $\beta_k = \beta_* + k\Delta\beta$, $k = 0, 1, \ldots, K$, $\Delta\beta = \frac{\beta^* - \beta_*}{K}$. Also, assume that $\gamma_k^n = \gamma(\beta_k, x, t_n)$ and $v^n = v(x, t^n)$.

Using the forward approximation $\frac{\partial v(x,s)}{\partial s} = \frac{v^{i+1} - v^i}{\Delta t} + O(\Delta t)$, we have:

$$\begin{aligned}\partial_t^\beta v^n &= \frac{1}{\Gamma(1-\beta)}\int_0^{t_n}(t_n - s)^{-\beta}\frac{\partial v(x,s)}{\partial s}ds \\ &= \frac{1}{\Gamma(1-\beta)}\sum_{i=0}^{n-1}\int_{t_i}^{t_{i+1}}(t_n - s)^{-\beta}\frac{\partial v(x,s)}{\partial s}ds\end{aligned}$$

$$= \frac{1}{\Delta t\Gamma(1-\beta)} \sum_{i=0}^{n-1} \int_{t_i}^{t_{i+1}} (t_n - s)^{-\beta} \left(v^{i+1} - v^i + O((\Delta t)^2) \right) ds$$

$$= \frac{1}{\Delta t\Gamma(1-\beta)} \sum_{i=0}^{n-1} \left(v^{i+1} - v^i \right) J_{i,n}^{\beta} + O(\Delta t), \tag{2.1}$$

where $J_{i,n}^{\beta} = \int_{t_i}^{t_{i+1}} (t_n - s)^{-\beta} ds$. Now for approximation ${}^{\gamma}\partial_t^* v^n$ we use the trapezoidal integration method as follows

$${}^{\gamma}\partial_t^* v^n = \frac{\Delta\beta}{2} \left(\gamma_0^n \partial_t^{\beta_0} v^n + 2 \sum_{k=1}^{K-1} \gamma_k^n \partial_t^{\beta_k} v^n + \gamma_K^n \partial_t^{\beta_K} v^n \right) + O((\Delta\beta)^2). \tag{2.2}$$

By substituting (2.1) in (2.2) we obtain

$${}^{\gamma}\partial_t^* v^n = \frac{\Delta\beta}{2\Delta t} \sum_{i=0}^{n-1} (v^{i+1} - v^i)\vartheta_i^n + O((\Delta\beta)^2 + (\Delta\beta)(\Delta t)), \tag{2.3}$$

where $\vartheta_i^n(x) = \eta_{i,0}^n(x) + 2 \sum_{k=1}^{K-1} \eta_{i,k}^n(x) + \eta_{i,K}^n(x)$, $\eta_{i,k}^n(x) = \frac{\gamma_k^n(x) J_{i,n}^{\beta_k}}{\Gamma(1-\beta_k)}$. By putting $t = t_{n+\frac{1}{2}}$ in (1.1) and using Crank–Nicolson method we get

$$v^{n+1} - v^n + \frac{\theta\Delta t}{2} \left({}^{\gamma}\partial_t^* v^{n+1} + {}^{\gamma}\partial_t^* v^n \right) - \frac{a\Delta t}{2} \left(v_{xx}^{n+1} + v_{xx}^n \right) + \frac{b\Delta t}{2} \left(v_x^{n+1} + v_x^n \right) + c\Delta t + O((\Delta t)^2) = \Delta t f(x, t_{n+\frac{1}{2}}). \tag{2.4}$$

Substituting (2.3) in (2.4) get

$$v^{n+1} + \frac{\theta\Delta\beta}{4}\vartheta_n^{n+1} v^{n+1} - \frac{a\Delta t}{2} v_{xx}^{n+1} + \frac{b\Delta t}{2} v_x^{n+1} = \left(1 + \frac{\theta\Delta\beta}{4}\vartheta_n^{n+1} \right) v^n - \frac{\theta\Delta\beta}{4} \sum_{i=0}^{n-1} (v^{i+1} - v^i) \left(\vartheta_i^{n+1} + \vartheta_i^n \right)$$
$$+ \frac{a\Delta t}{2} v_{xx}^n - \frac{b\Delta t}{2} v_x^n - c\Delta t + \Delta t f(x, t_{n+\frac{1}{2}}) + \varepsilon, \tag{2.5}$$

where $\varepsilon = O((\Delta t)(\Delta\beta)^2 + (\Delta\beta)(\Delta t)^2 + (\Delta t)^2)$. By eliminating the error term ε, the following semi-discrete numerical scheme is obtained:

$$V^{n+1} + \frac{\theta\Delta\beta}{4}\vartheta_n^{n+1} V^{n+1} - \frac{a\Delta t}{2} V_{xx}^{n+1} + \frac{b\Delta t}{2} V_x^{n+1} = \left(1 + \frac{\theta\Delta\beta}{4}\vartheta_n^{n+1} \right) V^n - \frac{\theta\Delta\beta}{4} \sum_{i=0}^{n-1} (V^{i+1} - V^i) \left(\vartheta_i^{n+1} + \vartheta_i^n \right)$$
$$+ \frac{a\Delta t}{2} V_{xx}^n - \frac{b\Delta t}{2} V_x^n - c\Delta t + \Delta t f(x, t_{n+\frac{1}{2}}), \tag{2.6}$$

where V_l^n represents the approximation of v_l^n.

Now we will introduce the collocation method based on Romanovski-Jacobi polynomials.

For the given integer numbers $M > 0$, $\rho > -1$ and $\varrho < -2M - \rho - 1$ a set containing $M + 1$ number of the Romanovski-Jacobi polynomials can be generated on $[0, \infty]$ using the below recursive relation [35]:

$$\begin{cases} R_{i+1}^{\rho,\varrho}(x) = (a_i^{\rho,\varrho} x - b_i^{\rho,\varrho}) R_i^{\rho,\varrho}(x) - c_i^{\rho,\varrho} R_{i-1}^{\rho,\varrho}(x), \quad 1 \le i \le M-1, \\ R_0^{\rho,\varrho}(x) = 1, \\ R_1^{\rho,\varrho}(x) = (v+2)x + p, \end{cases} \tag{2.7}$$

where

$$\begin{cases} a_i^{\rho,\varrho} = \frac{(h+1)(h+2)}{(i+1)(i+s+1)}, \\ b_i^{\rho,\varrho} = -\frac{(h+1)(k(i+1)+s(k+p))}{(i+1)(i+s+1)h}, \\ c_i^{\rho,\varrho} = \frac{(i+\rho)(i+\varrho)(h+2)}{(i+1)(i+s+1)h}, \end{cases}$$

and $k = 2i$, $h = k + s$, $s = \rho + \varrho$, and $p = \rho + 1$.

Also, we have [1]:

$$R_i^{\rho,\varrho}(x)=\sum_{k=0}^{i}\left(\begin{array}{c}-\rho-\varrho-i-1\\k\end{array}\right)\left(\begin{array}{c}\rho+i\\i-k\end{array}\right)(-x)^k, \tag{2.8}$$

with $R_i^{\rho,\varrho}(0)=\left(\begin{array}{c}\rho+i\\i\end{array}\right)$. The set $\{R_i^{\rho,\varrho}(x)\}_{i=0}^{i=M}$ creates a set of basis functions that are orthogonal with respect to the weight function $w^{\rho,\varrho}(x)=x^\rho(1+x)^\varrho$ over $[0,\infty)$, that is

$$\left\langle R_i^{\rho,\varrho}(x),R_j^{\rho,\varrho}(x)\right\rangle_{w^{\rho,\varrho}}=\int_0^\infty R_i^{\rho,\varrho}(x)R_j^{\rho,\varrho}(x)w^{\rho,\varrho}(x)dx=h_i^{\rho,\varrho}\delta_{i,j}, \tag{2.9}$$

where

$$\delta_{i,j}=\begin{cases}1, i=j,\\0, i\neq j,\end{cases}$$
$$h_i^{\rho,\varrho}=\|R_i^{\rho,\varrho}(x)\|_{w^{\rho,\varrho}}=-\frac{\Gamma(1+i+\rho)\Gamma(-i-\rho-\varrho)}{(1+2i+\rho+\varrho)i!\Gamma(-i-\varrho)}\geq 0.$$

Now we assume that

$$V^n(x)=\sum_{j=0}^{M}c_j^nR_j^{\rho,\varrho}(x). \tag{2.10}$$

By putting Equation (2.10) into (2.5), we get

$$\sum_{j=0}^{M}c_j^{n+1}P_j^{n,\rho,\varrho}(x)=r^n(x)+\varepsilon, \tag{2.11}$$

where

$$P_j^{n,\rho,\varrho}(x)=\left(1+\frac{\theta\Delta\beta}{4}\vartheta_n^{n+1}\right)R_j^{\rho,\varrho}(x)-\frac{a\Delta t}{2}R_j^{\prime\prime\rho,\varrho}(x)+\frac{b\Delta t}{2}R_j^{\prime\rho,\varrho}(x),$$
$$r^n(x)=\left(1+\frac{\theta\Delta\beta}{4}\vartheta_n^{n+1}\right)V^n-\frac{\theta\Delta\beta}{4}\sum_{i=0}^{n-1}\left(V^{i+1}-V^i\right)\left(\vartheta_i^{n+1}+\vartheta_i^n\right)+\frac{a\Delta t}{2}V_{xx}^n-\frac{b\Delta t}{2}V_x^n-c\Delta t+\Delta tf(x,t_{n+\frac{1}{2}}).$$

In order to establish homogeneous conditions, we put in Equation (2.10):

$$\sum_{j=0}^{M}c_j^{n+1}R_j^{\rho,\varrho}(\alpha_1)=0,\qquad\sum_{j=0}^{M}c_j^{n+1}R_j^{\rho,\varrho}(\alpha_2)=0 \tag{2.12}$$

By ignoring the error term ε in (2.11) and inserting the collocation points x_k into it, we obtain:

$$\sum_{j=0}^{M}c_j^{n+1}P_j^{n,\rho,\varrho}(x_k)=r^n(x_k),\quad k=1,2,\ldots,M-1, \tag{2.13}$$

such that $R_{M+1}^{\rho,\sigma}(x_k)=0$, $k=0,1,\ldots,M$. The matrix representation of Equations (2.12) and (2.13) will be as follows.

$$\mathbf{A}^n\mathbf{C}^{n+1}=\mathbf{R}^n,\quad n=0,1,\ldots,N-1, \tag{2.14}$$

where

$$\mathbf{A}^n = \begin{pmatrix} R_0^{\rho,\varrho}(\alpha_1) & R_1^{\rho,\varrho}(\alpha_1) & \cdots & R_M^{\rho,\varrho}(\alpha_1) \\ P_0^{n,\rho,\varrho}(x_1) & P_1^{n,\rho,\varrho}(x_1) & \cdots & P_M^{n,\rho,\varrho}(x_1) \\ P_0^{n,\rho,\varrho}(x_2) & P_1^{n,\rho,\varrho}(x_2) & \cdots & P_M^{n,\rho,\varrho}(x_2) \\ \vdots & \vdots & & \vdots \\ P_0^{n,\rho,\varrho}(x_{M-1}) & P_1^{n,\rho,\varrho}(x_{M-1}) & \cdots & P_M^{n,\rho,\varrho}(x_{M-1}) \\ R_0^{\rho,\varrho}(\alpha_2) & R_1^{\rho,\varrho}(\alpha_2) & \cdots & R_M^{\rho,\varrho}(\alpha_2) \end{pmatrix},$$

$$\mathbf{C}^n = \begin{pmatrix} c_0^n \\ c_1^n \\ c_2^n \\ \vdots \\ c_{M-1}^n \\ c_M^n \end{pmatrix}, \quad \mathbf{R}^n = \begin{pmatrix} 0 \\ r^n(x_1) \\ r^n(x_2) \\ \vdots \\ r^n(x_{M-1}) \\ 0 \end{pmatrix}.$$

Equation (2.14) allows us to find the coefficients of c_j^n, $j = 0, 1, \ldots, M$. To find the values of $\mathbf{C}^n$ for $n = 0$ using the initial condition (1.2) we have:

$$\sum_{j=0}^{M} c_j^0 R_j^{\rho,\varrho}(x) = v_0(x).$$

Therefore,

$$c_i^0 = \frac{1}{h_i} \int_0^{\infty} v_0(x) R_i^{\rho,\varrho}(x) w(x) dx, \quad i = 0, 1, \ldots, M. \tag{2.15}$$

Finally, the following equation is used to calculate the function values at (t_n, x_l) point:

$$V_l^n = \sum_{j=0}^{M} c_j^n R_j^{\rho,\varrho}(x_l). \tag{2.16}$$

The complete procedure for implementing the proposed method is outlined in Algorithm 1.

Algorithm 1 Numerical solution of problem (1.1)–(1.2) using Romanovski-Jacobi collocation methods.

Input T, α_1, α_2, β_*, β^*, σ, r, ρ, ϱ, θ, σ, r, M, N, L, K.
Input $v_0(x)$, $v_0'(x)$, $v_0''(x)$, $f(x,t)$, $\gamma(\beta, x, t)$, $w(x) = x^{\rho}(1+x)^{\varrho}$.
Compute t_n, x_l, β_k: $n = 0, 1, \ldots, N$, $l = 0, 1, \ldots, L$, $k = 0, 1, \ldots, K$.
Define Romanovski-Jacobi Polynomial $R_l^{\rho,\varrho}(x)$, $l = 0, 1, \ldots, M$ and xx:=roots of $R_{M+1}^{\rho,\varrho}(x)$ as functions.
Define a zero $L \times N$ matrix U and initialing that using initial condition (1.2).
Compute c_j^0, $j = 0, 1, \ldots, M$ using (2.15).
for $n = 0$ to $N - 1$ **do**
  Compute $\mathbf{A}^n$.
  Compute $\mathbf{R}^n$.
  Compute $\mathbf{C}^n$.
  for $l = 1$ to $L - 1$ **do**
    Compute $U(x_l, t_n) = \sum_{j=0}^{M} c_j^n R_j^{\rho,\varrho}(x_l)$, $U_x(x_l, t_n) = \sum_{j=0}^{M} c_j^n R_j'^{\rho,\varrho}(x_l)$, and $U_{xx}(x_l, t_n) = \sum_{j=0}^{M} c_j^n R_j''^{\rho,\varrho}(x_l)$.
  end for
end for

2.2. **Finite difference method.** By using central finite difference approximations for spatial approximation in (2.5) for $x = x_l$ we obtain

$$\begin{aligned} v_l^{n+1} + \frac{\theta\Delta\beta}{4}\vartheta_n^{n+1}(x_l)v_l^{n+1} - \frac{a\Delta t}{2(\Delta x)^2}(v_{l-1}^{n+1} - 2v_l^{n+1} + v_{l+1}^{n+1}) + \frac{b\Delta t}{4\Delta x}(v_{l+1}^{n+1} - v_{l-1}^{n+1}) \\ = \left(1 + \frac{\theta\Delta\beta}{4}\vartheta_n^{n+1}(x_l)\right)v_l^n - \frac{\theta\Delta\beta}{4}\sum_{i=0}^{n-1}(v_l^{i+1} - v_l^i)\left(\vartheta_i^{n+1}(x_l) + \vartheta_i^n(x_l)\right) \\ + \frac{a\Delta t}{2(\Delta x)^2}(v_{l-1}^n - 2v_l^n + v_{l+1}^n) - \frac{b\Delta t}{4\Delta x}(v_{l+1}^n - v_{l-1}^n) - c\Delta t + \Delta t f(x_l, t_{n+\frac{1}{2}}) + \varepsilon, \end{aligned} \tag{2.17}$$

where $v_l^n = v(x_l, t_n)$. Hence form (2.17) we obtain

$$-c_1 v_{l-1}^{n+1} + \Pi_{1,l}^n v_l^{n+1} - c_2 v_{l+1}^{n+1} = R_l^n + \varepsilon, \tag{2.18}$$

where

$$\begin{aligned} c_1 &= \frac{\Delta t}{2\Delta x}\left(\frac{a}{\Delta x} + \frac{b}{2}\right), \quad c_2 = \frac{\Delta t}{2\Delta x}\left(\frac{a}{\Delta x} - \frac{b}{2}\right), \\ \Pi_{1,l}^n &= 1 + \frac{\theta\Delta\beta}{4}\vartheta_n^{n+1}(x_l) + \frac{a\Delta t}{(\Delta x)^2}, \\ R_l^n &= c_1 v_{l-1}^n + \Pi_{2,l}^n v_l^n + c_2 v_{l+1}^n - \frac{\theta\Delta\beta}{4}\sum_{i=0}^{n-1}(v_l^{i+1} - v_l^i)\left(\vartheta_i^{n+1}(x_l) + \vartheta_i^n(x_l)\right) - c\Delta t + \Delta t f(x_l, t_{n+\frac{1}{2}}), \\ \Pi_{2,l}^n &= 1 + \frac{\theta\Delta\beta}{4}\vartheta_n^{n+1}(x_l) - \frac{a\Delta t}{(\Delta x)^2}. \end{aligned}$$

Therefore the numerical scheme where be obtained by elimination of error term ε in (2.18) as follows

$$-c_1 V_{l-1}^{n+1} + \Pi_{1,l}^n V_l^{n+1} - c_2 V_{l+1}^{n+1} = Rhs_l^n, \ n \geq 0, \tag{2.19}$$

where Rhs_l^n can be obtained by substituting V_l^n instead of v_l^n in R_l^n. From (2.19) we have the following system of linear equations to establish V_l^n, $l = 1, 2, \ldots, L$ and $n = 1, 2, \ldots, N$,

$$\begin{pmatrix} \Pi_{1,1}^n & -c_2 & & & \\ -c_1 & \Pi_{1,2}^n & -c_2 & & \\ & \ddots & \ddots & \ddots & \\ & & -c_1 & \Pi_{1,L-2}^n & -c_2 \\ & & & -c_1 & \Pi_{1,L-1}^n \end{pmatrix} \begin{pmatrix} V_1^{n+1} \\ V_2^{n+1} \\ \vdots \\ V_{L-2}^{n+1} \\ V_{L-1}^{n+1} \end{pmatrix} = \begin{pmatrix} Rhs_1^n \\ Rhs_2^n \\ \vdots \\ Rhs_{L-2}^n \\ Rhs_{L-1}^n \end{pmatrix}, \ n \geq 0. \tag{2.20}$$

3. Error analysis

3.1. **Convergence analysis.** In this subsection we assume that $E^n = v^n - V^n$, $E_x^n = v_x^n - V_x^n$, $E_{xx}^n = v_{xx}^n - V_{xx}^n$, $E_l^n = E^n(x_l)$, $(E_x)_l^n = (E_x^n)(x_l)$, $(E_{xx})_l^n = (E_{xx}^n)(x_l)$, $E_t^n = v_t^n - V_t^n$ and so on.

3.1.1. *Romanovski-Jacobi collocation method.* By subtracting (2.5) from (2.6) we get

$$\begin{aligned} \left(1 + \frac{\theta\Delta\beta}{4}\vartheta_n^{n+1}\right)E^{n+1} - \frac{a\Delta t}{2}E_{xx}^{n+1} + \frac{b\Delta t}{2}E_x^{n+1} = \left(1 + \frac{\theta\Delta\beta}{4}\vartheta_n^{n+1}\right)E^n - \frac{\theta\Delta\beta}{4}\sum_{i=0}^{n-1}\left(\vartheta_i^{n+1} + \vartheta_i^n\right)(E^{i+1} - E^i) \\ + \frac{a\Delta t}{2}E_{xx}^n - \frac{b\Delta t}{2}E_x^n + \varepsilon, \end{aligned} \tag{3.1}$$

Let $E^n = \sum_{j=0}^{M} c_j^n R_j^{\rho,\varrho}$, then from (3.1) we obtain

$$\left(1+\frac{\theta\Delta\beta}{4}\vartheta_n^{n+1}\right)\sum_{j=0}^{M}c_j^{n+1}R_j^{\rho,\varrho}-\frac{a\Delta t}{2}\sum_{j=0}^{M}c_j^{n+1}R_j''^{\rho,\varrho}+\frac{b\Delta t}{2}\sum_{j=0}^{M}c_j^{n+1}R_j'^{\rho,\varrho}$$
$$=\left(1+\frac{\theta\Delta\beta}{4}\vartheta_n^{n+1}\right)\sum_{j=0}^{M}c_j^{n}R_j^{\rho,\varrho}-\frac{\theta\Delta\beta}{4}\sum_{i=0}^{n-1}\left(\vartheta_i^{n+1}+\vartheta_i^{n}\right)\left(\sum_{j=0}^{M}c_j^{i+1}R_j^{\rho,\varrho}-\sum_{j=0}^{M}c_j^{i}R_j^{\rho,\varrho}\right)$$
$$+\frac{a\Delta t}{2}\sum_{j=0}^{M}c_j^{n}R_j''^{\rho,\varrho}-\frac{b\Delta t}{2}\sum_{j=0}^{M}c_j^{n}R_j'^{\rho,\varrho}+\varepsilon.$$

Or

$$\sum_{j=0}^{M}c_j^{n+1}\left(\left(1+\frac{\theta\Delta\beta}{4}\vartheta_n^{n+1}\right)R_j^{\rho,\varrho}-\frac{a\Delta t}{2}R_j''^{\rho,\varrho}+\frac{b\Delta t}{2}R_j'^{\rho,\varrho}\right)$$
$$=\sum_{j=0}^{M}\left(c_j^{n}\left(\left(1+\frac{\theta\Delta\beta}{4}\vartheta_n^{n+1}\right)R_j^{\rho,\varrho}+\frac{a\Delta t}{2}R_j''^{\rho,\varrho}-\frac{b\Delta t}{2}R_j'^{\rho,\varrho}\right)\right.$$
$$\left.-\sum_{i=0}^{n-1}\frac{\theta\Delta\beta}{4}\left(\vartheta_i^{n+1}+\vartheta_i^{n}\right)\left(c_j^{i+1}-c_j^{i}\right)R_j^{\rho,\varrho}\right)+\varepsilon. \tag{3.2}$$

Lemma 3.1. *[25] The Romanovski-Jacobi polynomials have derivatives of the form*

$$\frac{d^q}{dx^q}R_j^{\rho,\varrho}(x)=\sum_{k=0}^{j-q}C_{k,j}^{\rho,\varrho,q}R_k^{\rho,\varrho}(x), \tag{3.3}$$

where

$$C_{k,j}^{\rho,\varrho,q}=\frac{(-1)^q\Gamma(-\alpha_2)(\alpha_1+2k+1)\Gamma(1+j+\rho)}{\Gamma(-\alpha_1-k)\Gamma(1+\alpha_3)}$$
$$\times\sum_{n=0}^{j-k+q}\frac{(-1)^{n+1}\Gamma(n+\alpha_3+1)\Gamma(1-\alpha_1-2k-n)}{n!\Gamma(-\alpha_2-n-\alpha_4)\Gamma(\alpha_3+n+q+1)\Gamma(-j-n-\alpha_4+1)},$$

and $\alpha_1=\rho+\varrho$, $\alpha_2=j+\alpha_1$, $\alpha_3=\rho+k$, $\alpha_4=q+k$.

By substituting (3.3) in (3.2) we have

$$\sum_{j=0}^{M}c_j^{n+1}\left(\left(1+\frac{\theta\Delta\beta}{4}\vartheta_n^{n+1}\right)R_j^{\rho,\varrho}-\frac{a\Delta t}{2}\sum_{k=0}^{j-2}C_{k,j}^{\rho,\varrho,2}R_k^{\rho,\varrho}(x)+\frac{b\Delta t}{2}\sum_{k=0}^{j-1}C_{k,j}^{\rho,\varrho,1}R_k^{\rho,\varrho}(x)\right)$$
$$=\sum_{j=0}^{M}\left(c_j^{n}\left(\left(1+\frac{\theta\Delta\beta}{4}\vartheta_n^{n+1}\right)R_j^{\rho,\varrho}+\frac{a\Delta t}{2}\sum_{k=0}^{j-2}C_{k,j}^{\rho,\varrho,2}R_k^{\rho,\varrho}(x)-\frac{b\Delta t}{2}\sum_{k=0}^{j-1}C_{k,j}^{\rho,\varrho,1}R_k^{\rho,\varrho}(x)\right)\right.$$
$$\left.-\sum_{i=0}^{n-1}\frac{\theta\Delta\beta}{4}\left(\vartheta_i^{n+1}+\vartheta_i^{n}\right)\left(c_j^{i+1}-c_j^{i}\right)R_j^{\rho,\varrho}\right)+\varepsilon. \tag{3.4}$$

Now, assume that there are indexes ι and ς for which

$$\sum_{j=0}^{M}c_j^{n+1}\left(\left(1+\frac{\theta\Delta\beta}{4}\vartheta_n^{n+1}\right)R_j^{\rho,\varrho}-\frac{a\Delta t}{2}\sum_{k=0}^{j-2}C_{k,j}^{\rho,\varrho,2}R_k^{\rho,\varrho}+\frac{b\Delta t}{2}\sum_{k=0}^{j-1}C_{k,j}^{\rho,\varrho,1}R_k^{\rho,\varrho}\right)$$

$$\geq \sum_{j=0}^{M} c_j^{n+1} \left(\left(1 + \frac{\theta\Delta\beta}{4} \vartheta_n^{n+1} \right) - \frac{a\Delta t}{2} \sum_{k=0}^{j-2} C_{k,j}^{\rho,\varrho,2} + \frac{b\Delta t}{2} \sum_{k=0}^{j-1} C_{k,j}^{\rho,\varrho,1} \right) R_\iota^{\rho,\varrho}, \tag{3.5}$$

and

$$\sum_{j=0}^{M} \left(c_j^n \left(\left(1 + \frac{\theta\Delta\beta}{4} \vartheta_n^{n+1} \right) R_j^{\rho,\varrho} + \frac{a\Delta t}{2} \sum_{k=0}^{j-2} C_{k,j}^{\rho,\varrho,2} R_k^{\rho,\varrho} - \frac{b\Delta t}{2} \sum_{k=0}^{j-1} C_{k,j}^{\rho,\varrho,1} R_k^{\rho,\varrho} \right) - \sum_{i=0}^{n-1} \frac{\theta\Delta\beta}{4} \left(\vartheta_i^{n+1} + \vartheta_i^n \right) \left(c_j^{i+1} - c_j^i \right) R_j^{\rho,\varrho} \right)$$
$$\leq \sum_{j=0}^{M} \left(c_j^n \left(\left(1 + \frac{\theta\Delta\beta}{4} \vartheta_n^{n+1} \right) + \frac{a\Delta t}{2} \sum_{k=0}^{j-2} C_{k,j}^{\rho,\varrho,2} - \frac{b\Delta t}{2} \sum_{k=0}^{j-1} C_{k,j}^{\rho,\varrho,1} \right) - \sum_{i=0}^{n-1} \frac{\theta\Delta\beta}{4} \left(\vartheta_i^{n+1} + \vartheta_i^n \right) \left(c_j^{i+1} - c_j^i \right) \right) R_\varsigma^{\rho,\varrho}. \tag{3.6}$$

Then, from (3.4) we get

$$R_\iota^{\rho,\varrho} \sum_{j=0}^{M} c_j^{n+1} \left(\left(1 + \frac{\theta\Delta\beta}{4} \vartheta_n^{n+1} \right) - \frac{a\Delta t}{2} \sum_{k=0}^{j-2} C_{k,j}^{\rho,\varrho,2} + \frac{b\Delta t}{2} \sum_{k=0}^{j-1} C_{k,j}^{\rho,\varrho,1} \right)$$
$$\leq R_\varsigma^{\rho,\varrho} \sum_{j=0}^{M} \left(c_j^n \left(\left(1 + \frac{\theta\Delta\beta}{4} \vartheta_n^{n+1} \right) R_j^{\rho,\varrho} + \frac{a\Delta t}{2} \sum_{k=0}^{j-2} C_{k,j}^{\rho,\varrho,2} R_k^{\rho,\varrho} - \frac{b\Delta t}{2} \sum_{k=0}^{j-1} C_{k,j}^{\rho,\varrho,1} R_k^{\rho,\varrho} \right) \right.$$
$$\left. - \sum_{i=0}^{n-1} \frac{\theta\Delta\beta}{4} \left(\vartheta_i^{n+1} + \vartheta_i^n \right) \left(c_j^{i+1} - c_j^i \right) R_j^{\rho,\varrho} \right) + \varepsilon. \tag{3.7}$$

Let $R_\iota^{\rho,\varrho} \neq 0$, and

$$A_j^{n,\rho,\varrho} = \left(1 + \frac{\theta\Delta\beta}{4} \vartheta_n^{n+1} \right) - \frac{a\Delta t}{2} \sum_{k=0}^{j-2} C_{k,j}^{\rho,\varrho,2} + \frac{b\Delta t}{2} \sum_{k=0}^{j-1} C_{k,j}^{\rho,\varrho,1},$$
$$B_j^{n,\rho,\varrho} = \left(1 + \frac{\theta\Delta\beta}{4} \vartheta_n^{n+1} \right) + \frac{a\Delta t}{2} \sum_{k=0}^{j-2} C_{k,j}^{\rho,\varrho,2} - \frac{b\Delta t}{2} \sum_{k=0}^{j-1} C_{k,j}^{\rho,\varrho,1},$$
$$\lambda_i^n = \frac{\theta\Delta\beta}{4} \left(\vartheta_i^{n+1} + \vartheta_i^n \right).$$

Since $R_j^{\rho,\varrho}$s are bounded, from (3.7) we obtain

$$\sum_{j=0}^{M} \left(c_j^{n+1} A_j^{n,\rho,\varrho} - \frac{R_\varsigma^{\rho,\varrho}}{R_\iota^{\rho,\varrho}} c_j^n B_j^{n,\rho,\varrho} - \sum_{i=0}^{n-1} \lambda_i^n \left(c_j^{i+1} - c_j^i \right) \right) \leq \varepsilon. \tag{3.8}$$

Using Taylor expansion for c_j^{n+1}, we have

$$\sum_{j=0}^{M} \left(\left(c_j^n + O(\Delta t) \right) A_j^{n,\rho,\varrho} - \frac{R_\varsigma^{\rho,\varrho}}{R_\iota^{\rho,\varrho}} c_j^n B_j^{n,\rho,\varrho} - \sum_{i=0}^{n-1} \lambda_i^n \left(\left(c_j^i + O(\Delta t) \right) - c_j^i \right) \right) \leq \varepsilon. \tag{3.9}$$

And after simplification, the result is

$$\sum_{j=0}^{M} \left(O(\Delta t) \left(1 + \frac{\theta\Delta\beta}{4} \vartheta_n^{n+1} \right) + \left(1 + \frac{\theta\Delta\beta}{4} \vartheta_n^{n+1} \right) \left(1 - \frac{R_\varsigma^{\rho,\varrho}}{R_\iota^{\rho,\varrho}} \right) c_j^n \right.$$
$$- O(\Delta t) \frac{a\Delta t}{2} \sum_{k=0}^{j-2} C_{k,j}^{\rho,\varrho,2} - \frac{a\Delta t}{2} \sum_{k=0}^{j-2} C_{k,j}^{\rho,\varrho,2} \left(1 + \frac{R_\varsigma^{\rho,\varrho}}{R_\iota^{\rho,\varrho}} \right) c_j^n$$
$$\left. + O(\Delta t) \frac{b\Delta t}{2} \sum_{k=0}^{j-1} C_{k,j}^{\rho,\varrho,1} + \frac{b\Delta t}{2} \sum_{k=0}^{j-1} C_{k,j}^{\rho,\varrho,1} \left(1 + \frac{R_\varsigma^{\rho,\varrho}}{R_\iota^{\rho,\varrho}} \right) c_j^n - \sum_{i=0}^{n-1} \lambda_i^n O(\Delta t) \right) \leq \varepsilon. \tag{3.10}$$

Let Δt and $\Delta\beta$ tends to zero. Then from (3.10) we obtain

$$\left|\sum_{j=0}^{M}\left(1-\frac{R_{\varsigma}^{\rho,\varrho}}{R_{\iota}^{\rho,\varrho}}\right)c_j^n\right|=0. \tag{3.11}$$

This implies that $c_j^n\to 0$ and therefore $E^n\to 0$.

3.1.2. *Finite difference method.* By subtracting (2.18) from (2.19) and using Taylor expansions of V_{l-1}^n, V_{l+1}^n, v_{l-1}^n and v_{l+1}^n around (x_l,t^n) we have

$$\begin{aligned}&\left(1+\frac{\theta\Delta\beta}{4}\vartheta_n^{n+1}(x_l)\right)E_l^{n+1}+\frac{b\Delta t}{2}(E_x)_l^{n+1}-\frac{a\Delta t}{2}(E_{xx})_l^{n+1}+\frac{b\Delta t(\Delta x)^2}{12}(E_{xxx})_l^{n+1}-\frac{a\Delta t(\Delta x)^2}{24}(E_{xxxx})_l^{n+1}+\cdots\\&=\left(1+\frac{\theta\Delta\beta}{4}\vartheta_n^{n+1}(x_l)\right)E_l^{n}-\frac{b\Delta t}{2}(E_x)_l^{n}+\frac{a\Delta t}{2}(E_{xx})_l^{n}\\&-\frac{b\Delta t(\Delta x)^2}{12}(E_{xxx})_l^{n}+\frac{a\Delta t(\Delta x)^2}{24}(E_{xxxx})_l^{n}+\cdots-\frac{\theta\Delta\beta}{4}\sum_{i=0}^{n-1}\left(\vartheta_i^{n+1}(x_l)+\vartheta_i^{n}(x_l)\right)\left(E_l^{i+1}-E_l^{i}\right)+\varepsilon,\end{aligned} \tag{3.12}$$

and therefore

$$E_l^{n+1}=E_l^n-\frac{4\theta\Delta\beta}{4+\theta\Delta\beta\vartheta_n^{n+1}(x_l)}\sum_{i=0}^{n-1}\left(\vartheta_i^{n+1}(x_l)+\vartheta_i^{n}(x_l)\right)\left(E_l^{i+1}-E_l^{i}\right)+\frac{\varepsilon+O\left(\Delta t\right)}{4+\theta\Delta\beta\vartheta_n^{n+1}(x_l)}. \tag{3.13}$$

From (3.13) we can conclude that

$$|E_l^n|\le\sum_{k=1}^{n-1}\left|\frac{(4\theta\Delta\beta)^k}{\left(4+\theta\Delta\beta\vartheta_n^{n+1}(x_l)\right)^{k+1}}\right|+\left|\frac{(\varepsilon+O\left(\Delta t\right))}{4+\theta\Delta\beta\vartheta_n^{n+1}(x_l)}\right|, \tag{3.14}$$

Since $\vartheta_i^n(x_l)=O\left((\Delta t)^{1-\beta_K}\right)$ if $\Delta\beta\to 0$ then $|E_l^n|\le O\left(\Delta t+\Delta t\Delta x\right)$, $n=1,2,\ldots$.

3.2. **Stability Analysis.** In this subsection, we have added a comprehensive stability analysis for both the Finite Difference (FD) and the Romanovski–Jacobi Collocation (RJC) methods.

3.2.1. *Stability of the Collocation Method.*

Lemma 3.2 (Properties of the RJC Basis)**.** *The Romanovski–Jacobi polynomials $\{R_j^{\rho,\theta}(x)\}_{j=0}^M$ on $[0,\infty)$ with parameters $\rho>-1$, $\theta<-2M-\rho-1$ are orthogonal with respect to the weight function $w(x)=x^\rho(1+x)^\theta$:*

$$\int_0^\infty R_i^{\rho,\theta}(x)R_j^{\rho,\theta}(x)w(x)\,dx=h_i\delta_{ij},\quad h_i>0.$$

Moreover, their derivatives are bounded, and the mass matrix $\mathbf{M}$ *with entries $M_{ij}=\langle R_i,R_j\rangle_w$ is positive definite.*

Proof. Orthogonality follows from the definition of the Romanovski–Jacobi polynomials [1, 35]. The boundedness of derivatives is established in [25]. Since the basis is linearly independent and $w(x)>0$, the Gram matrix $\mathbf{M}$ is symmetric positive definite. □

Theorem 3.3 (Stability of the RJC Scheme)**.** *The implicit RJC scheme defined by (2.10)– (2.13) is unconditionally stable.*

Proof. Consider the semi-discrete equation (2.6) in weak form. Let $V^n(x)=\sum_{j=0}^M c_j^n R_j^{\rho,\theta}(x)$ and define the weighted L^2 inner product $\langle u,v\rangle_w=\int_{\alpha_1}^{\alpha_2}u(x)v(x)w(x)dx$. Multiplying (2.6) by a test function $\phi(x)=V^{n+1/2}(x)=\frac{1}{2}(V^{n+1}(x)+V^n(x))$ and integrating over $[\alpha_1,\alpha_2]$, we obtain:

$$\left\langle V^{n+1}-V^n,V^{n+1/2}\right\rangle_w+\frac{\theta\Delta\beta}{4}\left\langle\vartheta_n^{n+1}V^{n+1}+\vartheta_n^nV^n,V^{n+1/2}\right\rangle_w+\frac{\Delta t}{2}\left\langle\mathcal{L}_x(V^{n+1}+V^n),V^{n+1/2}\right\rangle_w=0, \tag{3.15}$$

where we have omitted the source and history terms for stability analysis. The operator $\mathcal{L}_x=-a\partial_{xx}+b\partial_x+c$.

We analyze each term:

(1) First term:

$$\left\langle V^{n+1}-V^n, V^{n+1/2}\right\rangle_w = \frac{1}{2}\left(\|V^{n+1}\|_w^2 - \|V^n\|_w^2\right),$$

where $\|V\|_w^2 = \langle V, V\rangle_w$.

(2) Second term: Since $\vartheta_n^{n+1}, \vartheta_n^n \geq 0$,

$$\left\langle \vartheta_n^{n+1}V^{n+1} + \vartheta_n^n V^n, V^{n+1/2}\right\rangle_w \geq \frac{1}{2}\left(\vartheta_n^{n+1}\|V^{n+1}\|_w^2 + \vartheta_n^n\|V^n\|_w^2\right) \geq 0.$$

(3) Third term: For the elliptic operator $\mathcal{L}_x$, integration by parts and the homogeneous Dirichlet boundary conditions yield:

$$\langle \mathcal{L}_x u, u\rangle_w = a\langle \partial_x u, \partial_x u\rangle_w + c\|u\|_w^2 + \langle b\partial_x u, u\rangle_w.$$

The last term can be bounded using Cauchy–Schwarz and Young's inequalities:

$$|\langle b\partial_x u, u\rangle_w| \leq |b|\|\partial_x u\|_w\|u\|_w \leq \frac{a}{2}\|\partial_x u\|_w^2 + \frac{b^2}{2a}\|u\|_w^2.$$

Therefore,

$$\langle \mathcal{L}_x u, u\rangle_w \geq \frac{a}{2}\|\partial_x u\|_w^2 + \left(c - \frac{b^2}{2a}\right)\|u\|_w^2.$$

Under the reasonable financial assumption $c = r > 0$ and for sufficiently large a (volatility), the quadratic form is coercive: there exists $\gamma > 0$ such that

$$\langle \mathcal{L}_x u, u\rangle_w \geq \gamma\|u\|_w^2.$$

Consequently,

$$\left\langle \mathcal{L}_x(V^{n+1}+V^n), V^{n+1/2}\right\rangle_w = \frac{1}{2}\langle \mathcal{L}_x(V^{n+1}+V^n), V^{n+1}+V^n\rangle_w \geq \frac{\gamma}{2}\|V^{n+1}+V^n\|_w^2.$$

Combining these estimates, we obtain:

$$\frac{1}{2}\left(\|V^{n+1}\|_w^2 - \|V^n\|_w^2\right) + \frac{\theta\Delta\beta}{8}\left(\vartheta_n^{n+1}\|V^{n+1}\|_w^2 + \vartheta_n^n\|V^n\|_w^2\right) + \frac{\gamma\Delta t}{4}\|V^{n+1}+V^n\|_w^2 \leq 0. \tag{3.16}$$

All terms on the left-hand side are non-negative except possibly the first difference. This implies:

$$\|V^{n+1}\|_w^2 \leq \|V^n\|_w^2.$$

Hence, the energy norm is non-increasing, and the scheme is unconditionally stable.

In the discrete setting, the collocation quadrature using the roots of $R_{M+1}^{\rho,\theta}(x)$ exactly integrates polynomials of degree up to $2M+1$ with respect to $w(x)$. Therefore, the discrete inner product preserves the coercivity and positivity properties, ensuring stability of the fully discrete system. □

3.2.2. *Stability of the Finite Difference Scheme.*

Theorem 3.4 (Stability of the FD Scheme)**.** *The implicit finite difference scheme defined by* (2.6) *is unconditionally stable in the von Neumann sense.*

Proof. Consider the constant-coefficient, homogeneous version of the semi-discrete FD scheme ((2.6) without source and history terms for stability analysis):

$$\left(1 + \frac{\theta\Delta\beta}{4}\vartheta_n\right)v_l^{n+1} - \frac{a\Delta t}{2}\delta_x^2 v_l^{n+1} + \frac{b\Delta t}{2}\Delta_x v_l^{n+1} = \left(1 + \frac{\theta\Delta\beta}{4}\vartheta_n\right)v_l^n + \frac{a\Delta t}{2}\delta_x^2 v_l^n - \frac{b\Delta t}{2}\Delta_x v_l^n, \tag{3.17}$$

where

$$\delta_x^2 v_l = \frac{v_{l-1} - 2v_l + v_{l+1}}{(\Delta x)^2}, \quad \Delta_x v_l = \frac{v_{l+1} - v_{l-1}}{2\Delta x}.$$

We assume periodic or homogeneous Dirichlet boundary conditions. Substituting a Fourier mode $v_l^n = \xi^n e^{i\omega l\Delta x}$ (where ξ is the amplification factor and ω the wave number) yields:

$$\delta_x^2 v_l^n = -\frac{4}{(\Delta x)^2}\sin^2\left(\frac{\omega\Delta x}{2}\right)v_l^n,$$
$$\Delta_x v_l^n = i\frac{\sin(\omega\Delta x)}{\Delta x}v_l^n.$$

Define

$$\lambda = \frac{4a}{(\Delta x)^2}\sin^2\left(\frac{\omega\Delta x}{2}\right), \quad \mu = \frac{b\sin(\omega\Delta x)}{\Delta x}.$$

Then Eq. (3.17) becomes:

$$\left(1+\frac{\theta\Delta\beta}{4}\vartheta_n + \frac{\Delta t}{2}\lambda - i\frac{\Delta t}{2}\mu\right)\xi = \left(1+\frac{\theta\Delta\beta}{4}\vartheta_n - \frac{\Delta t}{2}\lambda + i\frac{\Delta t}{2}\mu\right).$$

Hence, the amplification factor is:

$$\xi(\omega) = \frac{1+\frac{\theta\Delta\beta}{4}\vartheta_n - \frac{\Delta t}{2}\lambda + i\frac{\Delta t}{2}\mu}{1+\frac{\theta\Delta\beta}{4}\vartheta_n + \frac{\Delta t}{2}\lambda - i\frac{\Delta t}{2}\mu}.$$

Let $A = 1+\frac{\theta\Delta\beta}{4}\vartheta_n$, $B = \frac{\Delta t}{2}\lambda$, $C = \frac{\Delta t}{2}\mu$. Then

$$|\xi|^2 = \frac{(A-B)^2+C^2}{(A+B)^2+C^2}.$$

Since $a = \sigma^2/2 > 0$, we have $\lambda > 0$ for $\omega \neq 0$, and by definition $\vartheta_n \geq 0$. Therefore, $A > 0$ and $B \geq 0$. It follows that $A + B > A - B \geq 0$, so the numerator is strictly less than the denominator for all $\omega \neq 0$, giving $|\xi(\omega)| < 1$. For $\omega = 0$, $|\xi(0)| = 1$. Thus, the scheme is unconditionally stable. □

Both numerical methods are unconditionally stable due to their fully implicit formulation.

4. Numerical experiments

In this section, we study the numerical results of the implementation of the presented methods on three examples. In this study, the MATLAB software was applied within the framework of MATLAB R2017a software (V9.2.0.538062, 64-bit (win64), License Number: 416517, MathWorks Inc., Natick, MA) running on a HP Probook 4530s Laptop (Intel Core i5 2410 M Processor 2.30 GHz, 8 GB of RAM, 64-bit) PC.

To measure the convergence of the numerical method, we use the norm of difference of two successive steps of the approximate solutions as follows

$$\left\|V^N - V^{N+1}\right\|_\infty := \max_{0\leq l\leq L}\left|V^N(x_l,T) - V^{N+1}(x_l,T)\right|.$$

In all numerical examples we assume that $T = 1$, $\alpha_1 = 0$, $\alpha_2 = 1$, and $v_0(x) = \sin(\pi x)$.

In this work, two numerical approaches are employed:

RJC: Romanovski-Jacobi Collocation method, a spectral approach that uses orthogonal polynomials as basis functions.

FD: Finite Difference method, a classical discretization technique based on local Taylor expansions.

Both methods are applied for spatial discretization of the distributed-order fractional Black-Scholes equation, while the time derivative is approximated using an L1-type scheme.

Example 4.1. Let $\beta_* = 0.2$, $\beta^* = 0.8$, $r = 0.05$, $\sigma = 0.5$, $\theta = 1$, $\rho = 1$, $\varrho = -25$, $M = 10$, and $\gamma(\beta,x,t) = 0.01(\beta+1)\sqrt{(x+1)(t+1)}$.

This choice represents a smooth, separable function that depends linearly on the fractional order β and varies mildly in space and time. It serves as a baseline to verify the implementation and demonstrate the method's accuracy against a constructed exact solution.

The exact solution is assumed to be $v(x,t) = (1+t)\sin(\pi x)$ and $f(x,t)$ can be obtained from exact solution.

The numerical and exact solutions for $N = 20$, $L = 20$, and $K = 20$ are shown in Figure 1. In addition, Figure 2 shows the absolute errors in all mesh points using $N = 20$, $L = 20$, and $K = 20$. Table 3 reports the difference of two successive steps of the approximate solutions for different values of L and N for $K = 20$ and $\theta = 1$. Table 4 presents the temporal convergence of the RJC and FD methods for Example 1 with a polynomial density function. The spatial resolution is fixed $M = 10$ for RJC and $L = 100$ for FD. The results confirm first-order convergence (≈ 1) for both methods, which is consistent with the theoretical order of the L1-type scheme for the fractional derivative. The error for the RJC method is systematically smaller than that of the FD method at each time step. Table 5 reports the spatial convergence for Example 1, with a fixed temporal resolution ($N = 1000$). Both methods exhibit second-order convergence (≈ 2) in space. The superior accuracy of the RJC method is also evident in this table.

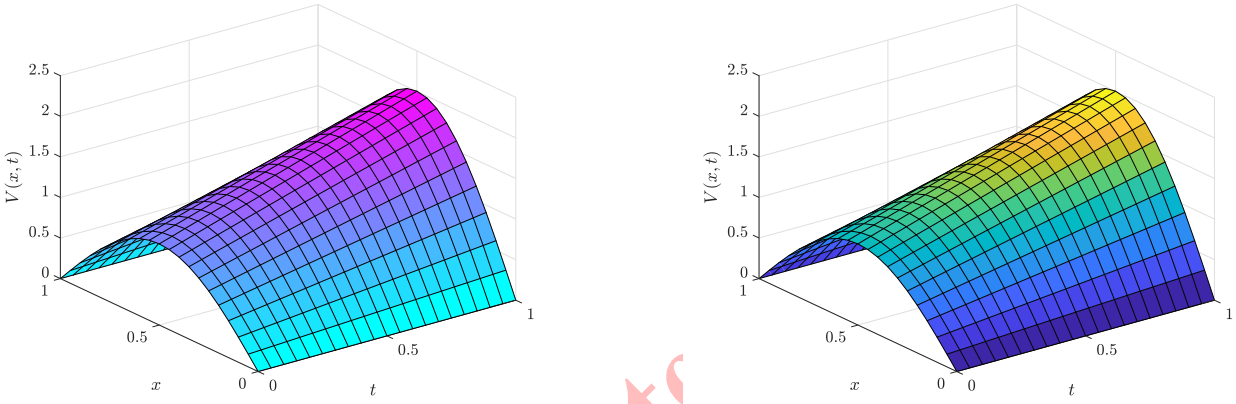

FIGURE 1. Numerical solution using Romanovski-Jacobi collocation method (left) and the finite difference method (right) for all mesh points in Example 4.1 with $N = 20$, $L = 20$ and $K = 20$.

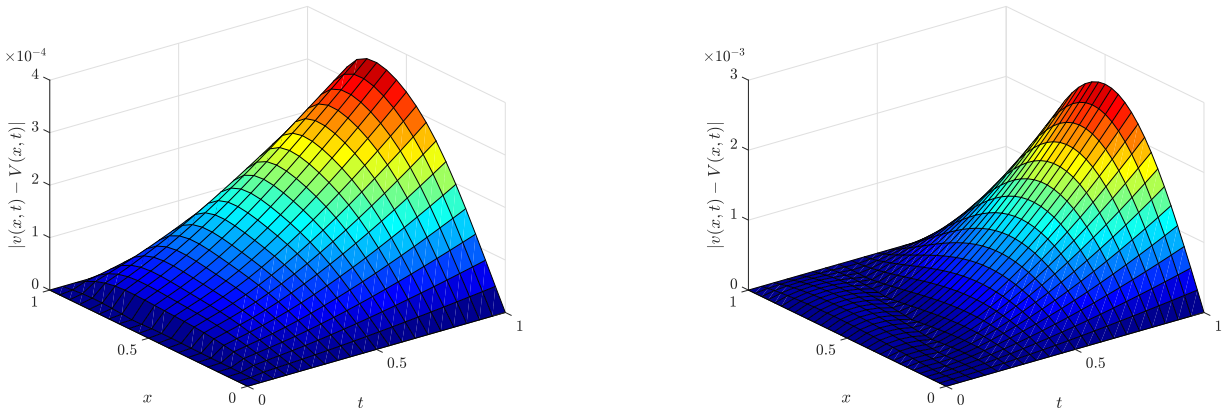

FIGURE 2. The absolute errors for all mesh points in Example 4.1 with $N = 20$, $L = 20$ and $K = 20$ by Romanovski-Jacobi collocation method (left) and finite difference method (right).

TABLE 3. The difference of two successive steps of the approximate solutions with $K = 20$ in Example 4.1.

N	Romanovski-Jacobi collocation method		Finite difference method	
	$\|V^N - V^{N+1}\|_\infty$	CPU time	$\|V^N - V^{N+1}\|_\infty$	CPU time
1	$1.507050e-03$	5.551	$7.619586e-02$	1.152
5	$1.176713e-04$	11.515	$1.886442e-02$	2.554
10	$4.008993e-05$	24.951	$2.998643e-03$	12.541
15	$2.133567e-05$	45.148	$1.171031e-03$	22.354
20	$1.363447e-05$	68.951	$7.499334e-04$	41.861
30	$7.253977e-06$	89.756	$5.212626e-04$	63.843
40	$4.637064e-06$	117.350	$3.341602e-04$	96.174
50	$3.278077e-06$	161.254	$1.877646e-04$	114.582

TABLE 4. Temporal convergence for Example 4.1.

N	Δt	RJC error	Order	FD error	Order
10	0.1	$3.823156e{-3}$	–	$1.124732e{-2}$	–
20	0.05	$1.915482e{-3}$	0.997	$5.618450e{-3}$	1.001
40	0.025	$9.557130e{-4}$	1.003	$2.801245e{-3}$	1.004
80	0.0125	$4.771021e{-4}$	1.002	$1.398876e{-3}$	1.002

TABLE 5. Spatial convergence for Example 4.1.

L (FD) / M (RJC)	Δx	RJC error	Order	FD error	Order
10 / 5	0.1	$6.314520e{-4}$	–	$5.253142e{-3}$	–
20 / 10	0.05	$1.582340e{-4}$	1.997	$1.312850e{-3}$	2.001
40 / 15	0.025	$3.952180e{-5}$	2.001	$3.281450e{-4}$	2.000
80 / 20	0.0125	$9.873210e{-6}$	2.001	$8.198720e{-5}$	2.001

Example 4.2. Let $\rho = 1$, $\varrho = -25$, $M = 10$, $\beta_* = 0.2$, $\beta^* = 0.8$, $r = 0.05$, $\sigma = 0.5$, and $f = 0$ (see [47])

$$\gamma(\beta, x, t) = \frac{1}{\sqrt{2\pi}\delta(x,t)} \exp\left(-\frac{(\beta - \bar{\beta})^2}{2(\delta(x,t))^2}\right),$$

where $\bar{\beta} = (\beta_l + \beta_r)/2$, $\delta(x,t) = \sqrt{10^{-3}(x+1)(t+1)}$.

This form is motivated by applications where the fractional order is concentrated around a mean value $\bar{\beta}$ with a small, spatially and temporally varying variance δ^2, a model relevant for capturing multi-scale memory effects with a dominant scale.

In Figure 3, the numerical solutions (using Romanovski-Jacobi collocation method) of problem (1.1)–(1.2) are depicted using $N = L = K = 50$ and $\theta = 1$. Also, the numerical solutions in $t = T$ for different values of θ are shown in Figure 4, for $N = 50$, $L = 50$, and $K = 50$. The difference of two successive steps of the approximate solutions for different values of L and N for $K = 20$ and $\theta = 1$ are tabulated in Table 6. Table 7 shows the temporal convergence for Example 2 with a Gaussian density. The RJC method maintains its advantage in accuracy, yielding a smaller estimated error. Table 8 details the spatial convergence for Example 2. The results confirm second-order convergence (≈ 2) for the spatial discretization in both methods. The slightly higher convergence rate reported for the FD method may be attributed to the nature of the error estimation.

Example 4.3. In this example we assume that

$$\gamma(\beta, x, t) = \frac{x+1}{\beta^*}\left(\frac{\beta}{\beta^*}\right)^x,$$

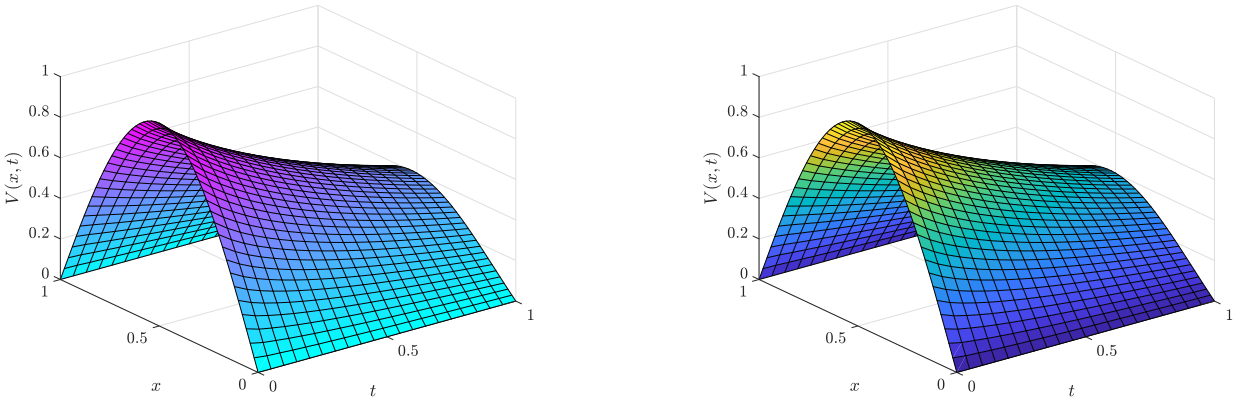

FIGURE 3. Numerical solution using Romanovski-Jacobi collocation method (left) and the finite difference method (right) for all mesh points in Example 4.2 with $\theta = 1$, $N = 50$, $L = 50$ and $K = 50$.

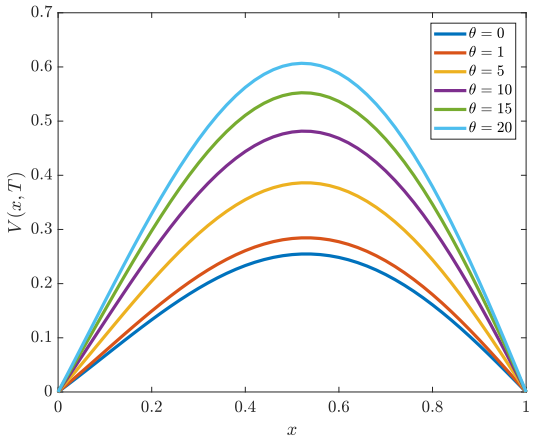

FIGURE 4. Numerical solutions (using Romanovski-Jacobi collocation method) for different values of θ for Example 4.2 with $t = T$, $N = L = K = 50$.

TABLE 6. The difference of two successive steps of the approximate solutions with $K = 20$ in Example 4.2.

N	Romanovski-Jacobi collocation method		Finite difference method	
	$\|V^N - V^{N+1}\|_\infty$	CPU time	$\|V^N - V^{N+1}\|_\infty$	CPU time
1	$3.308077e-03$	8.254	$3.876492e-02$	2.351
5	$6.480129e-04$	15.364	$1.018208e-02$	3.354
10	$2.661171e-04$	32.254	$2.333271e-03$	15.325
15	$1.534061e-04$	53.245	$1.217126e-03$	32.256
20	$1.028125e-04$	77.305	$9.107313e-04$	49.971
30	$5.793123e-05$	102.650	$7.253662e-04$	71.952
40	$3.836248e-05$	130.254	$5.534415e-04$	105.309
50	$2.780195e-05$	183.296	$3.913414e-04$	128.351

TABLE 7. Temporal convergence for Example 4.2.

N	Δt	RJC error	Order	FD error	Order
20	0.05	$1.034872e{-4}$	–	$9.114520e{-4}$	–
40	0.025	$5.148630e{-5}$	1.008	$4.552310e{-4}$	1.002
80	0.0125	$2.571240e{-5}$	1.002	$2.276540e{-4}$	1.000

TABLE 8. Spatial convergence for Example 4.2.

L (FD) / M (RJC)	Δx	RJC error	Order	FD error	Order
20 / 5	0.05	$2.441250e{-4}$	–	$1.224580e{-3}$	–
40 / 10	0.025	$6.101800e{-5}$	2.001	$3.042130e{-4}$	2.009
80 / 15	0.0125	$1.524500e{-5}$	2.001	$7.601200e{-5}$	2.001

and $a = 0.1$, $\beta_* = b = c = 0$, $\beta^* = 0.8$, $\rho = 1$, $\varrho = -25$, $M = 10$, and $f(x,t) = 0$ (see [47]).

This function introduces a non-separable and potentially singular (depending on x) structure. It tests the algorithm's ability to handle density functions that are not symmetric and that weight lower or higher fractional orders differently across the spatial domain.

The numerical solutions for $N = L = K = 30$ and $\theta = 1$ are shown in Figure 5 (using Romanovski-Jacobi collocation method). Also, the option price V in $t = T$ for different values of θ are shown in Figure 6 (using Romanovski-Jacobi collocation method) for $N = 30$, $L = 30$, and $K = 30$. The difference of two successive steps of the approximate solutions for different values of L and N for $K = 30$ and $\theta = 1$ are reported in Table 9. Table 10 presents the temporal convergence results for Example 3 with an exponential density. Again, first-order convergence (≈ 1) is observed for both methods. The difference in error between the two methods is smaller in this example, indicating the robust performance of the FD method for this type of density function. Table 11 shows the spatial convergence for Example 3. Both methods clearly demonstrate second-order convergence. The absolute error of the RJC method is approximately half that of the FD method, underscoring the accuracy advantage of the spectral method even for nonlinear density functions.

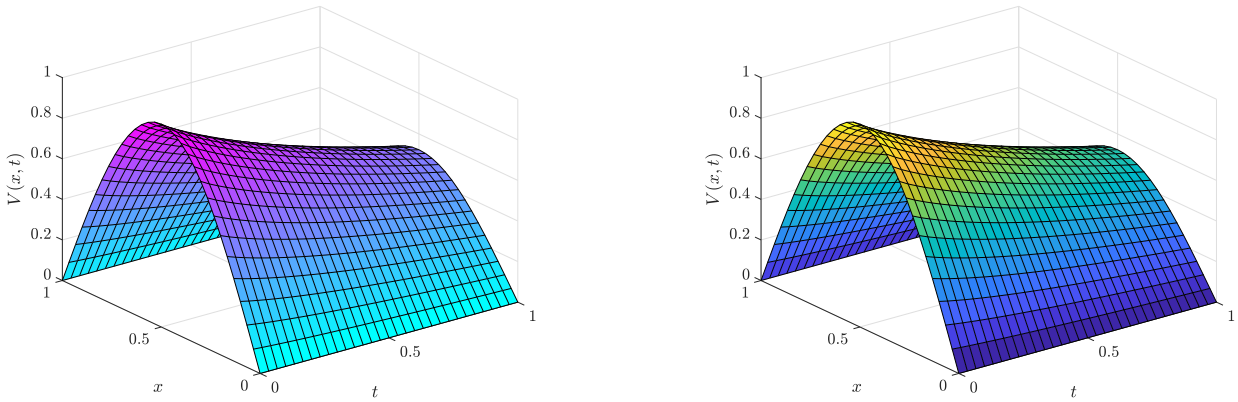

FIGURE 5. Numerical solution using Romanovski-Jacobi collocation method (left) and the finite difference method (right) for all mesh points in Example 4.3 with $\theta = 1$, $N = 30$, $L = 30$ and $K = 30$.

RJC (Romanovski-Jacobi Collocation): Delivers higher accuracy due to its spectral basis, ideal for problems requiring precise solutions or involving complex boundaries. Best used when computational cost per step is less critical than solution fidelity.

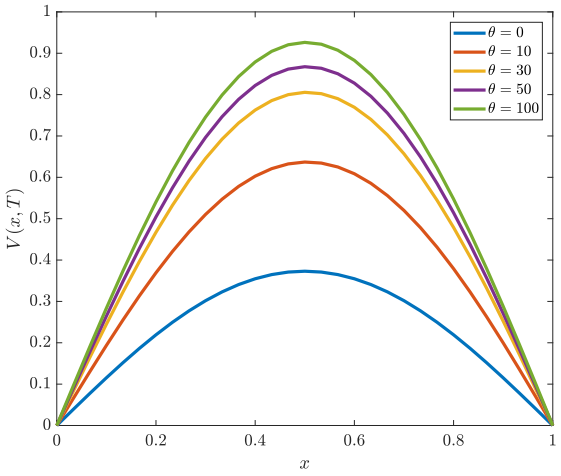

FIGURE 6. Numerical solutions for different values of θ for Example 4.3 with $t = T$, $N = L = K = 30$.

TABLE 9. The difference of two successive steps of the approximate solutions with $K = 30$ in Example 4.3.

N	Romanovski-Jacobi collocation method		Finite difference method	
	$\|V^N - V^{N+1}\|_\infty$	CPU time	$\|V^N - V^{N+1}\|_\infty$	CPU time
1	$2.966207e-03$	7.366	$3.876492e-02$	2.015
5	$5.538093e-04$	14.365	$4.011518e-03$	3.125
10	$2.244126e-04$	29.821	$1.016076e-03$	14.256
15	$1.295187e-04$	49.430	$4.534264e-04$	30.570
20	$8.721549e-05$	75.910	$3.039708e-04$	46.981
30	$4.972480e-05$	98.147	$2.178506e-04$	68.002
40	$3.331798e-05$	124.782	$1.451652e-04$	101.254
50	$1.441276e-05$	175.853	$9.221441e-05$	126.682

TABLE 10. Temporal convergence for Example 4.3.

N	Δt	RJC error	Order	FD error	Order
20	0.05	$8.721540e-5$	–	$3.041250e-4$	–
40	0.025	$4.361230e-5$	1.000	$1.520840e-4$	1.000
80	0.0125	$2.180120e-5$	1.000	$7.601250e-5$	1.000

TABLE 11. Spatial convergence for Example 4.3.

L (FD) / M (RJC)	Δx	RJC error	Order	FD error	Order
20 / 5	0.05	$1.812540e-4$	–	$4.531240e-4$	–
40 / 10	0.025	$4.521300e-5$	2.003	$1.131250e-4$	2.002
80 / 15	0.0125	$1.130120e-5$	2.001	$2.828120e-5$	2.000

FD (Finite Difference): Provides greater computational efficiency and implementation simplicity, making it suitable for long simulations, real-time applications, or extensive parameter studies where speed and ease-of-use are prioritized.

Choice Guidance: Select RJC for accuracy-driven tasks on moderate grids; choose FD for efficiency-focused applications or for problems with less regular solutions. Both methods are robust and stable across various distributed-order density functions.

4.1. **Sensitivity Analysis.** In this subsection we conducted a comprehensive sensitivity analysis to investigate the robustness of our numerical methods to variations in the fractional order parameters and the distributed-order density function. The distributed-order operator ∂_t^* integrates over a continuum of fractional orders $\beta \in [\beta_*, \beta^*]$, weighted by $\gamma(\beta, x, t)$. The accuracy of the numerical approximation depends critically on the discretization of this integral. Therefore, the methods are expected to be sensitive to:

(1) The fractional order range $[\beta_*, \beta^*]$: A wider interval increases the stiffness and memory requirements of the problem.
(2) The density function $\gamma(\beta, x, t)$: Functions with sharp peaks, discontinuities, or high gradients pose a challenge to the quadrature rule used in Eq. (2.2).

We performed a detailed parameter study on Example 2 (Gaussian density) because its mean $\bar{\beta}$ and variance δ^2 are easily tunable. We measured the impact on two key outputs:

- Solution Accuracy: The L_∞ error relative to a highly refined reference solution (obtained with $N = L = K = 160$).
- Numerical Stability: Monitored by the maximum absolute value in the solution matrix to detect unbounded growth.

All tests used a base resolution of $N = 40$, $L = 40$, and $K = 40$, varying one parameter at a time. The results are summarized in Tables 12, 13, and 14.

TABLE 12. Sensitivity to the fractional order range $[\beta_*, \beta^*]$. Parameters: $\bar{\beta} = 0.5$, $\delta^2 = 0.01$.

β_*	β^*	Range	RJC Error	RJC Stable?	FD Error	FD Stable?
0.1	0.5	0.4	4.21×10^{-5}	Yes	1.89×10^{-4}	Yes
0.1	0.9	0.8	5.04×10^{-5}	Yes	2.15×10^{-4}	Yes
0.3	0.7	0.4	4.32×10^{-5}	Yes	1.92×10^{-4}	Yes
0.0	1.0	1.0	8.76×10^{-5}	Yes	4.01×10^{-4}	Yes

TABLE 13. Sensitivity to the concentration (variance δ^2) of the Gaussian distribution. Parameters: $[\beta_*, \beta^*] = [0.2, 0.8]$, $\bar{\beta} = 0.5$.

δ^2	RJC Error	RJC Stable?	FD Error	FD Stable?
0.001	3.98×10^{-5}	Yes	1.76×10^{-4}	Yes
0.01	4.15×10^{-5}	Yes	1.84×10^{-4}	Yes
0.05	5.62×10^{-5}	Yes	2.45×10^{-4}	Yes
0.1	1.12×10^{-4}	Yes	5.11×10^{-4}	Yes

TABLE 14. Sensitivity to the type of density function $\gamma(\beta, x, t)$. Parameters: $[\beta_*, \beta^*] = [0.2, 0.8]$, $N = L = K = 40$.

Density Type	Parameters	RJC Error	RJC Stable?	FD Error	FD Stable?
Gaussian	$\bar{\beta} = 0.5, \delta^2 = 0.01$	4.15×10^{-5}	Yes	1.84×10^{-4}	Yes
Uniform	$\gamma(\beta) = 1$	3.89×10^{-5}	Yes	1.70×10^{-4}	Yes
Exponential	$\gamma(\beta) = e^{-10(\beta - \beta_*)}$	4.87×10^{-5}	Yes	2.23×10^{-4}	Yes
Delta-like	Very narrow Gaussian ($\delta^2 = 0.0001$)	6.54×10^{-5}	Yes	3.01×10^{-4}	Yes

The analysis reveals several important insights:

(1) Robust Stability: Crucially, both methods remained numerically stable across all tested parameter variations. This confirms the robustness of the implicit time-stepping formulation.
(2) Controlled Sensitivity to Range: As shown in Table 12, expanding the fractional order range $[\beta_*, \beta^*]$ (especially including limits near 0 or 1) increases the error for both methods, as expected. The RJC method consistently shows lower sensitivity (smaller error increase) than the FD method.
(3) Impact of Distribution Shape: Table 13 indicates that as the Gaussian distribution becomes more concentrated (smaller δ^2), the error slightly decreases because the problem behaves more like a single-order fractional PDE. Table 14 confirms the methods' reliability for different density types. The "delta-like" case, approximating a single fractional order, presents the largest error due to the increased challenge for the distributed-order quadrature.
(4) Superior Robustness of RJC: In all scenarios, the Romanovski-Jacobi collocation (RJC) method demonstrated lower absolute errors and less sensitivity to parameter changes compared to the finite difference (FD) method. Its spectral accuracy provides a buffer against variations in the model's parameters.

Conclusion and Recommendation for Practitioners: While the methods are mathematically sensitive to the fractional order parameters as any distributed-order solver must be our proposed schemes handle this sensitivity in a stable and controlled manner. For real-world applications:

- A parameter study similar to the one presented here is recommended when calibrating the model to market data.
- The RJC method is preferable if the density function γ is expected to be sharply peaked or if high fidelity is critical.
- The FD method remains a reliable and efficient choice for smoother distributions and exploratory analysis.

5. Conclusion

In this work, the research successfully tackles the generalized distributed-order time-fractional Black-Scholes equation through the application of an implicit method. By employing collocation method based on Romanovski-Jacobi polynomials and finite difference techniques to approximate both time and spatial derivatives, we have streamlined the computational process, making it more efficient. The numerical results validate the precision of our approaches, demonstrating its robustness in solving financial models. Furthermore, our findings contribute to the broader understanding of numerical methods in financial mathematics, offering a reliable tool for practitioners and researchers alike. The implications of this work extend beyond theoretical interest, providing practical solutions for real-world financial problems. Future research could explore the application of this method to other complex financial equations, potentially enhancing the accuracy and efficiency of financial modeling and risk assessment.

The unconditionally stable implicit schemes developed here enable reliable long-term financial simulations, such as pricing long-dated path-dependent options or calculating credit exposure profiles, where capturing persistent market memory is crucial. Future work will focus on calibrating the density function $\gamma(\beta, x, t)$ to market option surfaces and extending the model to multi-asset portfolios.

These methods are particularly well-suited for modeling volatility clustering and long-range market memory. The unconditional stability of our implicit schemes makes long-term financial simulations feasible (e.g., for pricing long-dated options or calculating credit exposure). The FD method is recommended for fast computations (e.g., real-time pricing or large-scale Monte Carlo simulations), while the RJC method is ideal for high-accuracy tasks (e.g., pricing complex exotic options or benchmark validation).

References

[1] H. AboGabal, M. A. Zaky, R. M. Hafez, and E. H. Doha, *On Romanovski-Jacobi polynomials and their related approximation results*, Numerical Methods for Partial Differential Equations, *36*(6) (2020), 1982–2017.
[2] Y. E. Aghdam, H. Mesgarani, A. Adl, and B. Farnam, *The convergence investigation of a numerical scheme for the tempered fractional Black-Scholes model arising European double barrier option*, Computational Economics, *61*(2) (2023), 513–528.

[3] Y. E. Aghdam, A. Neisy, and A. Adl, *Simulating and pricing CAT bonds using the spectral method based on chebyshev basis*, Computational Economics, *63*(1) (2024), 423–435.

[4] H. Aminikhah and S. J. Alavi, *A new approach to using the cubic B-spline functions to solve the Black-Scholes equation*, JNRM, (2019), 71–80.

[5] L. Angermann and S. Wang, *Convergence of a fitted finite volume method for the penalized Black-Scholes equation governing European and American Option pricing*, Numerische Mathematik, *106*(1) (2007), 1–40.

[6] C. Bayer, P. Friz, and J. Gatheral, *Pricing under rough volatility*, Quantitative Finance, *16*(6) (2016), 887–904.

[7] F. Black and M. Scholes, *The pricing of options and corporate liabilities*, Journal of political economy, *81*(3) (1973), 637–654.

[8] Á. Cartea, *Derivatives pricing with marked point processes using tick-by-tick data*, Quantitative Finance, *13*(1) (2013), 111–123.

[9] Á. Cartea, & del-Castillo-Negrete, D. *Fractional diffusion models of option prices in markets with jumps*, Physica A: Statistical Mechanics and its Applications, *374*(2) (2007), 749–763.

[10] Z. Cen and A. Le, *A robust finite difference scheme for pricing American put options with singularity-separating method*, Numerical Algorithms, *53*(4) (2010), 497–510.

[11] Z. Cen and A. Le, *A robust and accurate finite difference method for a generalized Black-Scholes equation*, Journal of Computational and Applied Mathematics, *235*(13) (2011), 3728–3733.

[12] Y. Chen, H. Yu, X. Meng, X. Xie, M. Hou, and J. Chevallier, *Numerical solving of the generalized Black-Scholes differential equation using Laguerre neural network*, Digital Signal Processing, *112* (2021), 103003.

[13] R. Company, L. Jódar, and J. R. Pintos, *A consistent stable numerical scheme for a nonlinear option pricing model in illiquid markets*, Mathematics and Computers in Simulation, *82*(10) (2012), 1972–1985.

[14] R. Cont and O. Tankov, *Financial modelling with jump processes*, Chapman and Hall/CRC, 2003.

[15] J. C. Cox, S. A. Ross, and M. Rubinstein, *Option pricing: A simplified approach*, Journal of financial Economics, *7*(3) (1979), 229–263.

[16] J. P. Fouque, G. Papanicolaou, R. Sircar, and K. Solna, *Multiscale stochastic volatility asymptotics*, Multiscale Modeling & Simulation, *2*(1) (2003), 22–42.

[17] J. Gatheral, T. Jaisson, and M. Rosenbaum, *Volatility is rough*, In Commodities, Chapman and Hall/CRC, (2022), 659–690.

[18] A. Golbabai, O. Nikan, and T. Nikazad, *Numerical analysis of time fractional Black-Scholes European option pricing model arising in financial market*, Computational and Applied Mathematics, *38*(4) (2019), 173.

[19] S. L. Heston, *A Closed-Form Solution for Options with Stochastic Volatility, with Applications to Bond and Currency Options*, Review of Financial Studies *6* (1993).

[20] J. Hull and A. White, *The use of the control variate technique in option pricing*, Journal of Financial and Quantitative analysis, *23*(3) (1988), 237–251.

[21] G. Jumarie, *Stock exchange fractional dynamics defined as fractional exponential growth driven by (usual) Gaussian white noise. Application to fractional Black-Scholes equations*, Insurance: Mathematics and Economics, *42*(1) (2008), 271–287.

[22] M. K. Kadalbajoo, L. P. Tripathi, and P. Arora, *A robust nonuniform B-spline collocation method for solving the generalized Black-Scholes equation*, IMA Journal of Numerical Analysis, *34*(1) (2014), 252–278.

[23] M. K. Kadalbajoo, L. P. Tripathi, and A. Kumar, *A cubic B-spline collocation method for a numerical solution of the generalized Black-Scholes equation*, Mathematical and Computer Modelling, *55*(3-4) (2012), 1483–1505.

[24] K. Kazmi, *A second order numerical method for the time-fractional Black-Scholes European option pricing model*, Journal of Computational and Applied Mathematics, *418* (2023), 114647.

[25] A. Lachin, M. A. Abdelkawy, and S. Sathasivam, *An efficient collocation method based on Legendre and Romanovski polynomials for solving Riesz distributed fractional differential equations*, Alexandria Engineering Journal, *129* (2025), 312–328.

[26] D. C. Lesmana and S. Wang, *An upwind finite difference method for a nonlinear Black-Scholes equation governing European option valuation under transaction costs*, Applied Mathematics and Computation, *219*(16) (2013), 8811–8828.

[27] A. Lipton, *Mathematical methods for foreign exchange: A financial engineer's approach*, 2001.
[28] M. Magdziarz, *Black-Scholes formula in subdiffusive regime*, Journal of Statistical Physics, *136*(3) (2009), 553–564.
[29] M. M. Meerschaert and A. Sikorskii, *Stochastic models for fractional calculus* (Vol. 43). Walter de Gruyter GmbH & Co KG, 2019.
[30] M. Mehdizadeh Khalsaraei, M. M. Rashidi, A. Shokri, H. Ramos, and P. Khakzad, *A Nonstandard Finite Difference Method for a Generalized Black-Scholes Equation*, Symmetry, *14*(1) (2022), 141.
[31] L. Meng and M. Wang, *Comparison of Black-Scholes formula with fractional Black-Scholes formula in the foreign exchange option market with changing volatility*, Asia-Pacific Financial Markets, *17*(2) (2010), 99–111.
[32] R. C. Merton, *Theory of Rational Option Pricing*, Bell Journal of Economics and Management Science, *4* (1) (1973) 141–183.
[33] R. C. Merton, *Option pricing when underlying stock returns are discontinuous*, Journal of financial economics, *3*(1-2) (1976), 125–144.
[34] H. Mesgarani, A. Adl, and A. Y. Esmaeelzade, *Approximate price of the option under discretization by applying fractional quadratic interpolation*, 2022.
[35] J. Nazari, M. H. Heydari, M. Hosseininia, *Romanovski-Jacobi polynomials for the numerical solution of multi-dimensional multi-order time fractional telegraph equations*, Results in Physics, *53* (2023), 106937.
[36] S. M. Nuugulu, F. Gideon, and K. C. Patidar, *A robust numerical solution to a time-fractional Black-Scholes equation*, Advances in Difference Equations, *2021*(1) (2021), 123.
[37] J. Oliva-Maza and M. Warma, *Introducing and solving generalized Black-Scholes PDEs through the use of functional calculus*, Journal of Evolution Equations, *23*(1) (2023), 10.
[38] H. Payandehdoost Masouleh and M. Esmailzadeh, *An efficient numerical method based on cubic B–splines for the time–fractional Black–Scholes European option pricing model*. Journal of Mathematical Modeling, *12*(3) (2024), 405–417.
[39] D. Prathumwan and K. Trachoo, *On the solution of two-dimensional fractional Black-Scholes equation for European put option*, Advances in Difference Equations, *2020*(1) (2020), 146.
[40] S. C. S. Rao, *Numerical solution of generalized Black-Scholes model*, Applied Mathematics and Computation, *321* (2018), 401–421.
[41] P. Roul and V. P. Goura, *A new higher order compact finite difference method for generalised Black-Scholes partial differential equation: European call option*, Journal of Computational and Applied Mathematics, *363* (2020), 464–484.
[42] S. R. Saratha, G. Sai Sundara Krishnan, M. Bagyalakshmi, and C. P. Lim, *Solving Black-Scholes equations using fractional generalized homotopy analysis method*, Computational and Applied Mathematics, *39*(4) (2020), 262.
[43] E. Scalas, R. Gorenflo, and F. Mainardi, *Fractional calculus and continuous-time finance*. Physica A: Statistical Mechanics and its Applications, *284*(1-4) (2000), 376–384.
[44] R. Valkov, *Fitted finite volume method for a generalized Black-Scholes equation transformed on finite interval*, Numerical Algorithms, *65*(1) (2014), 195–220.
[45] S. Wang, *A novel fitted finite volume method for the Black-Scholes equation governing option pricing*, IMA Journal of Numerical Analysis, *24*(4) (2004), 699–720.
[46] W. Wyss, *The fractional Black-Scholes equation*, Fract. Cal. Appl. Anal., *3*(1) (2000), 51–61.
[47] M. Zhang, J. Jia, and X. Zheng, *Numerical approximation and fast implementation to a generalized distributed-order time-fractional option pricing model*, Chaos, Solitons & Fractals, *170* (2023), 113353.
[48] M. Zhang and G. F. Zhang, *Fast solution method and simulation for the 2D time-space fractional Black-Scholes equation governing European two-asset option pricing*, Numerical Algorithms, *91*(4) (2022), 1559–1575.
[49] H. Zhang, M. Zhang, F. Liu, and M. Shen, *Review of the fractional Black-Scholes equations and their solution techniques*, Fractal and Fractional, *8*(2) (2024), 101.